
Accelerated Sparse Neural Training: A Provable and Efficient Method to Find $N:M$ Transposable Masks

Itay Hubara^{*12} Brian Chmiel^{*12} Moshe Island² Ron Banner² Seffi Naor³ Daniel Soudry¹
{ihubara, bchmiel, misland, rbanner}@habana.ai
naor@cs.technion.ac.il
daniel.soudry@gmail.com

Abstract

Recently, researchers proposed pruning deep neural network weights (DNNs) using an $N : M$ fine-grained block sparsity mask. In this mask, for each block of M weights, we have at least N zeros. In contrast to unstructured sparsity, $N : M$ fine-grained block sparsity allows acceleration in actual modern hardware. So far, this was used for DNN acceleration at the inference phase. First, we suggest a method to convert a pretrained model with unstructured sparsity to a $N : M$ fine-grained block sparsity model, with little to no training. Then, to also allow such acceleration in the training phase, we suggest a novel transposable-fine-grained sparsity mask where the same mask can be used for both forward and backward passes. Our transposable mask ensures that both the weight matrix and its transpose follow the same sparsity pattern; thus the matrix multiplication required for passing the error backward can also be accelerated. We discuss the transposable constraint and devise a new measure for mask constraints, called mask-diversity (MD), which correlates with their expected accuracy. Then, we formulate the problem of finding the optimal transposable mask as a minimum-cost-flow problem and suggest a fast linear approximation that can be used when the masks dynamically change while training. Our experiments suggest 2x speed-up with no accuracy degradation over vision and language models. A reference implementation can be found at https://github.com/papers-submission/structured_transposable_masks.

^{*}Equal contribution ¹Electrical Engineering Department - Technion, Haifa, Israel ²Habana Labs – An Intel company, Caesarea, Israel ³Computer Science Department - Technion, Haifa, Israel. Correspondence to: Itay Hubara <ihubara@habana.ai>.

1. Introduction

Deep neural networks (DNNs) have established themselves as the first-choice tool for a wide range of applications, including computer vision and natural language processing. However, their impressive performance comes with a price of extensive infrastructure costs as they may contain trillions of parameters (Fedus et al., 2021) and require thousands of petaflops (Brown et al., 2020) for the training process. For this reason, compression of DNNs training and inference process is a leading research topic of researchers in the academy and industry. The main techniques of compression includes quantization (Banner et al., 2018a; Nahshan et al., 2019), knowledge distillation (Hinton et al., 2015) and pruning (Han et al., 2015; Li et al., 2017).

Pruning DNNs is one of the most popular and widely studied methods to improve DNN resource efficiency. The different pruning methods can be categorized into two different groups: unstructured and structured pruning. While the former can achieve a very high compression ratio, it usually fails in reducing the computation footprint in modern hardware. On the other hand, structured pruning methods, such as block (Wen et al., 2016) or filter (Li et al., 2017) pruning, are more hardware friendly. Unfortunately, these methods usually fail to keep original accuracy for high compression ratios (Renda et al., 2020a).

Recently, Nvidia (Nvidia, 2020) announced the A100 GPU, containing sparse tensor cores which are able to accelerate fine-grained sparse matrix multiplication. The sparse tensor cores in A100 enable a 2x acceleration of regular matrix multiplication in DNNs, $Y = WX$, where W and X are weight and input matrices, respectively. The only requirement is that W would have a fine-grained 2:4 sparsity structure, i.e. out of every four contiguous elements in W , two are pruned. Consequently, models with unstructured sparsity, in general, would suffer a severe degradation in accuracy when forced to adhere to a $N : M$ sparsity structure. In our first contribution of this paper (Section 3)

- We analyze the setting of converting a pretrained model

with unstructured sparsity to $N : M$ sparsity structure. We suggest two light methods that together can prevent the degradation when less than 10% of the active weights must be set to zero.

However, more commonly, only a pretrained dense model is given. Therefore, Nvidia (2020) suggested a two-fold scheme for pruning a dense model: (a) Define a fixed mask which for every weight tensor prunes the two smallest magnitude elements out of a block of four contiguous elements, and (b) retrain with the masked weights using original training schedule. Indeed, Nvidia (2020) approach is very appealing for the common case where a pretrained dense model is given.

While Nvidia (2020) method works well on many models, a pretrained model is not always given. Thus, Zhou et al. (2021) suggested a method that trains from scratch a model with N:M fine-grained mask, using a sparse-refined straight-through estimator (SR-STE). Similar to the quantize-aware-training method (Hubara et al., 2017) they maintain a dense copy of the weights and prune it every iteration while keeping the gradients oblivious to that process using the straight-through estimator (Bengio et al., 2013). Since the mask dynamically change while training they suggest adding an extra weight decay on the masked (i.e. pruned) elements to reduce the mask changes during the training process.

The rest of the paper focuses on accelerating sparse training in the two settings detailed above (starting from pretrained model or starting from scratch). Training DNNs requires three matrix multiplications per layer: one for the forward pass, one for the backward pass, and the last for the weight update. Both the forward and the backward matrix-multiplications involve the weight matrix W , yet the methods suggested in Zhou et al. (2021); Nvidia (2020) accelerate only the forward pass matrix-multiplication:

$$Y = WX. \quad (1)$$

Therefore, the current methods use the sparse tensor cores to accelerate approximately a third of the total computation during training. We note, that for the backward pass, the sparse tensor cores cannot be utilized, even if W has fine-grained sparsity. This is because the transposed matrix W^T is used for the backward pass multiplication:

$$\frac{\partial \text{Loss}}{\partial X} = \frac{\partial \text{Loss}}{\partial Y} W^T \quad (2)$$

and W^T does not generally have an N:M fine-grained sparsity structure, even if W has such structure.

We propose a novel $N : M$ transposable-fine-grained sparsity mask, where the same mask can be used for both the forward and backward passes. Our suggested mask contains only $M - N$ non-zero elements for every contiguous

M elements — simultaneously in both W and W^T . In Fig. 1 we emphasize the difference between previously suggested methods of $N : M$ fine-grained structured pruning (Zhou et al., 2021; Nvidia, 2020), which accelerates only the forward pass, and our suggested method, which is able to accelerate the backward pass as well.

In this setting,

- For the case of pretrained dense models, we suggest a novel method for training models with the $N : M$ transposable-fine-grained sparsity mask, exploiting modern sparse core tensors to allow acceleration of the forward and backward passes. Our method uses a novel algorithm to determine the optimal transposable-mask using a reduction to the min-cost-flow problem (Section 4).
- For the case where the model is trained from scratch, we define an approximation scheme with an (almost) linear (in input-size) time complexity that produces a mask whose l_1 -norm is within a factor of 2 from the optimal mask (Section 4.2).
- We suggest a new measure called mask diversity, which, to the best of our knowledge, provides the first connection between the mask constraints and network accuracy for a fixed sparsity ratio (Section 5).

2. Related work

Pruning of neural networks weights has been extensively investigated, starting with classical methods in the late 1980s (Janowsky, 1989; Mozer & Smolensky, 1989a;b; Karnin, 1990) and amounting to dozens of papers published in recent years. Since DNNs are generally over-parameterized, pruning the weights reduces their memory footprint. In special cases, when the sparsity mask has a specific pattern, it has the potential to reduce computation footprint as well. The most common practice is to prune a pretrained dense model so it will be sparse at deployment. Since the pretrained dense model accuracy is known, one can tune the sparsity level to ensure comparable accuracy for the sparse model. Recently, a new line of research that aims to train sparse models from scratch (Gray et al., 2017; Dettmers & Zettlemoyer, 2019; Evci et al., 2020) has emerged. Their goal is to train models that cannot fit into currently available hardware. Next, we would briefly overview the structured, unstructured, and sparse-training-from-scratch categories.

Unstructured pruning removes individual elements of the matrix, aiming for high total sparsity, while being agnostic to the location of the pruned elements. Standard pruning methods are based on different criteria, such as

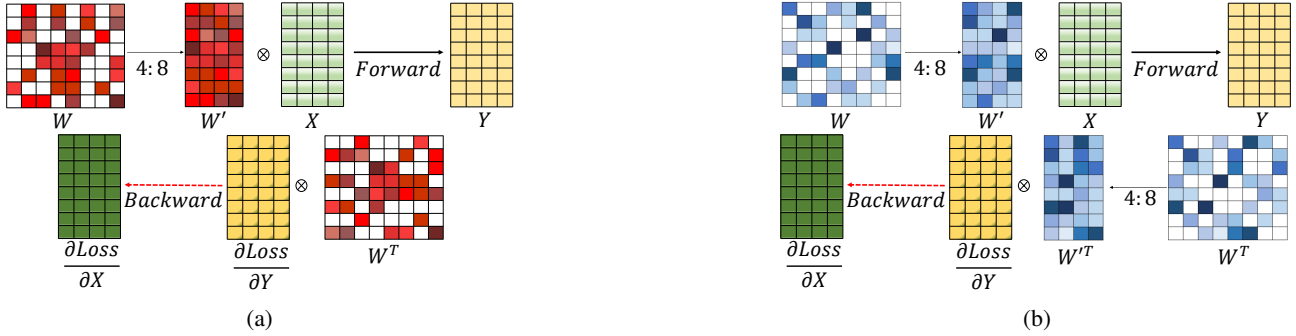


Figure 1. (a): A 4:8 structured fine-grained pruning as used in Zhou et al. (2021); Nvidia (2020), capable of accelerating with sparse core tensors only the forward pass. (b): The suggested 4:8 transpose structured fine-grained pruning capable of accelerating with sparse core tensors the forward and backward passes.

magnitude (Han et al., 2015), approximated L_0 regularization (Louizos et al., 2018) or connection sensitivity (Lee et al., 2019). Recent methods (Frankle & Carbin, 2018) suggested to train a dense network until convergence, extract the required mask (“winning ticket”), and use the original training regime to re-train the active weights from their original initialization or final values (Renda et al., 2020b) using the original training schedule. These methods are able to achieve over 80% sparsity on ResNet50- ImageNet dataset (Renda et al., 2020b). Despite the high sparsity ratio that can be achieved with these methods, modern hardware cannot efficiently utilize such a form of sparsity for reducing the computation resources (Nvidia, 2020).

Structured pruning removes weights in specific location based patterns, which are more useful for hardware acceleration. Such methods can be applied at the level of channels or layers. For example, Li et al. (2017) removed the channels with the lower norm, Luo et al. (2017) pruned channels according to the effect on the activation of the following layer, and Wen et al. (2016) split the filters into multiple groups and applied a group Lasso regularization. All methods are natively supported in both hardware and software, as they effectively change the model structure by reducing channels or groups. Yet, no method was able to achieve a reasonable accuracy with sparsity levels higher than 50%. As observed by Liu et al. (2018), filter pruning of a pretrained dense over-parameterized model is rarely the best method to obtain an efficient final model. Thus, here the structured pruning serves mostly as a DNN architecture search for the optimal compact model (Tan et al., 2019; Wu et al., 2019). Our work is most closely related to Zhou et al. (2021), which is the first work that attempted training with a fine-grained $N : M$ structured sparsity mask, as explained above.

Sparse training from scratch Gray et al. (2017) was the first to introduce this approach for NLP tasks. They investigated a fixed mask in which blocks of size $N \times N$

are either pruned (i.e., all elements are set to zero) or not. They implemented dedicated kernels for GPUs with several blocks sizes ($N=8,16,32$) and reported their results. While they managed to achieve slightly less than x2 training speedup for 50% sparsity, they observed high speedups as the sparsity level increases (x5 for 90% sparsity level). They initiated their masks using predefined schemes and fixed them throughout the training process. As expected, this method resulted in accuracy degradation if one does not expand the model size. Thus several researchers (Bellec et al., 2017; Mocanu et al., 2018; Mostafa & Wang, 2019; Dettmers & Zettlemoyer, 2019; Evci et al., 2020) tried to enable dynamic mask changes during the training process. All methods focused on unstructured sparsity and aimed to enable training large models on hardware with memory limitations. The first to introduce this approach was Bellec et al. (2017) which essentially applied a random walk in parameter space. At initialization connections are assigned a pre-defined sign at random; if during optimization the sign is flipped the weight would be pruned and a new weight will be activated at random (i.e., regrow). Sparse Evolutionary Training (SET) (Mocanu et al., 2018) proposed a simpler scheme where they pruned weights based on their magnitude. Dettmers & Zettlemoyer (2019) replaced the random regrow with a per-layer mean-momentum-magnitude redistribution. Evci et al. (2020) expanded Mocanu et al. (2018) mask initialization scheme to convolution kernels and suggested pruning and regrowing based on dense gradients, calculated once every several iterations. As opposed to these approaches, Zhou et al. (2021) does not aim to reduce the model memory footprint and keeps a dense weight matrix. At each iteration, they re-calculate the mask and use it to obtain a pruned copy of the weights, which then serves for the forward and backward pass. Therefore, this method is most relevant when a pretrained dense model is not given, and one wishes to obtain a fine-grained sparse model for inference.

3. From unstructured to structured sparsity

Most DNN pruning methods focus on unstructured pruning, which reduces the memory footprint. However, current hardware implementations suggest that, unless very high sparsity levels are achieved, the model cannot be accelerated at all. Thus, commonly, the weights are simply decompressed before multiplication. Forcing structured sparsity on a model that was trained without structured sparsity, leads to a severe accuracy degradation as several bits of the mask may change to satisfy the structured sparsity requirements.

In this section, we study the probability that an unstructured mask would not violate any $N : M$ constraint (Nvidia, 2020). We then discuss two light methods to bridge the gap when a sparse model is given but the hardware does not support its structure.

Probability for violating the $N : M$ constraint in unstructured sparsity. Let $X = \{x_1, x_2, \dots, x_M\}$ be a block of independent and identically distributed random variables. Assume that with a probability ρ , x_i can be pruned without accuracy degradation (i.e., unstructured pruning). In this section, we consider a general form of block sparsity in which, for a block of size M , at least N values could be pruned.

Define X to be $N : M$ sparse if this M sized block has at least N values that can be pruned without harming accuracy. The probability of having a $N : M$ sparse block is given by the binomial distribution and so

$$P(X \text{ is } N : M \text{ sparse}) = \sum_{i \geq N} \binom{M}{i} \cdot \rho^i \cdot (1 - \rho)^{M-i} \quad (3)$$

This probability goes to 1 as $M \rightarrow \infty$ if $N/M = c < \rho$. In Fig. 2 we demonstrate this Eq. (3) for $\rho = 0.5$.

To force a given sparse model to have a fine grained $N : M$ sparsity, we need to make sure that N out of every M contiguous elements are zero. Therefore, as in Nvidia (2020), in each block we prune N weights with the lowest magnitude (including any zero weights, e.g., non-active). Forcing this pattern on an existing unstructured mask might remove active (non-zero) weights, i.e., flipping some of the mask values from one to zero. We named those required flips, *pattern-violations*. Removing active weights without re-training tends to severely degrade the model accuracy. To demonstrate the problem we used an unstructured sparse pretrained ResNet-50 model ($\rho = 0.86$) and set the $N : M$ structure per-layer, based on Eq. (3), such that the probability for a pattern-violation would be equal or less than a given percentage. Here we used a block size of $M = 8$. As can be seen in Fig. 3, without any optimization even a 1% pattern-violation results in severe degradation. Next, we detail two light methods to boost the accuracy.

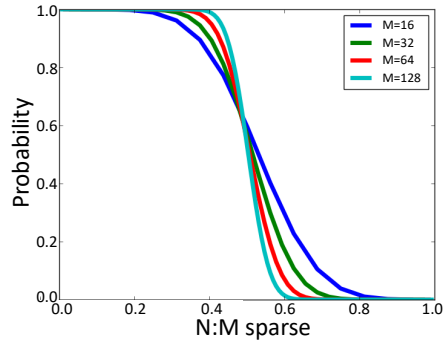


Figure 2. Eq. (3) for $\rho = 0.5$ and various block sizes M . We have a sharp (“phase”) transition at $N/M = \rho$. Specifically, (i) when $N/M \leq \rho$ we have a probability larger than 0.5 that the sampled block is $N : M$ sparse; (ii) when $N/M \geq \rho$ this probability quickly decreases to zero. As block size M increases this phase-transition gets sharper. As expected, when $M \rightarrow \infty$, unstructured sparsity satisfies the structured constraints, and we expect it to display the phase transition precisely at the critical point ρ .

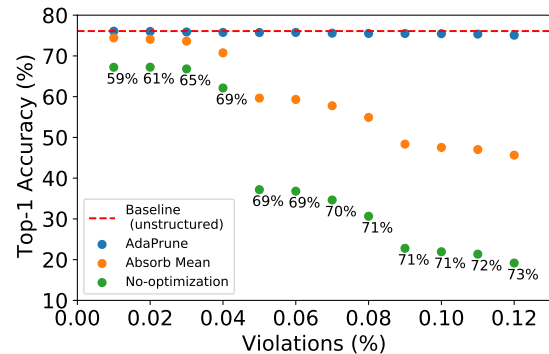


Figure 3. Top-1 accuracy vs. percent of constraints violated. The numbers next to the baseline samples represents the sparsity level of the refined model.

Pruning bias fix: Several works (Banner et al., 2018b; Finkelstein et al., 2019; Hubara et al., 2020) reported that it is important to fix the bias introduced when quantizing the model. We build on those results and suggest absorbing the mean of the N pruned weights into the $M - N$ non zeroed weights. As can be seen in Fig. 3 this simple fix, by itself, greatly boosts accuracy.

AdaPrune Recently, several works (Hubara et al., 2020; Nagel et al., 2020) suggested small fast fine-tuning techniques for post-training quantization. These techniques replace the heavy full model training with a fast per-layer optimization which requires only a few iterations to converge. While each method applies a different optimization

technique, they all aim to reduce the discrepancy between the quantized and full-precision layer outputs. We adapted parallel-AdaQuant (Hubara et al., 2020) technique which optimizes (using a small calibration set) the weights and quantization parameters to reduce the pre-activation reconstruction error, measured via mean squared-error per-layer. We adjusted their objective to the pruning problem

$$\min_{W'} \|WX - (\text{Mask} \odot W')X\|_2, \quad (4)$$

where W is the original weight layer, W' is the weight layer we aim to find, X is the output of the previous activation layer, "Mask" is the weight sparsity mask, and \odot is a component-wise product. We named this method AdaPrune. In our experiments we used 1000 images from the ImageNet training set as a calibration set. As can be seen in Fig. 3, AdaPrune is capable of correcting the remaining error and obtain less than 1% degradation from the original unstructured-sparse model counterpart. We argue that with AdaPrune, we can potentially adapt any generic mask to the hardware at hand, thus elevate the need to retrain the model.

However, usually a pretrained unstructured sparse model is not given. When starting from a dense model (thus having 50% pattern-violation) we get 2.3% degradation using AdaPrune. We discuss and extend those experiments in Appendix A.1. Thus, retraining is required to prevent such degradation. In the next sections, we'll discuss two scenarios: The first is the common case when a pretrained dense model is given. The second is a more challenging scenario in which one aims to train with a sparse mask from scratch.

4. Computing transposable sparsity masks

In general, training DNNs requires three matrix multiplications per layer. The first multiplication is required for the forward propagation between the weights and activation (Eq. (1)). The other two multiplications are used for the backward and update phases. The backward phase calculates the gradients of the loss function with respect to the input of the neural layer. This is done by recursively passing the error, from the last layer to the first (Eq. (2)). Note that the backward phase uses the transposed weights matrix. Hence, accelerating the backward phase requires the transposed weight matrix to adhere to the hardware required pattern (e.g., $N : M$ fine-grained sparsity).

In this section, we aim to tackle this issue by presenting a novel $N : M$ transposable fine-grained sparsity mask, where the same mask can be used to accelerate both forward and backward passes. The required mask, contains only $M - N$ non-zero elements for every contiguous M elements in both in W and W^T simultaneously. We formulate the problem and suggest two methods to generate the transposable mask: the first one trains from a dense model using a min-cost flow procedure, and the second one trains

from scratch, using an approximation algorithm that allows a more efficient training.

4.1. Problem formulation

First, we provide an integer-programming (IP) formulation for finding an optimal transposable fine-grained mask. Let us consider a block of size $M \times M$ in a weight matrix W . Our goal is to maximize the l_1 norm of W after masking N elements in each row and column.

We formulate the problem as an integer program. Define a binary indicator variable $I_{i,j}$, where $I_{i,j} = 1$ if and only if the element $W_{i,j}$ is part of the chosen mask, otherwise $I_{i,j} = 0$. The integer program is as follows:

$$\begin{aligned} & \text{Maximize} && \sum_{i,j=0}^{M-1} |W_{i,j}| \cdot I_{ij} \\ \text{S.t} & && \sum_j I_{ij} = N, \quad \forall i \in \{0, \dots, M-1\} \\ & && \sum_i I_{ij} = N, \quad \forall j \in \{0, \dots, M-1\} \\ & && I_{i,j} \in \{0, 1\}, \quad \forall i, j \in \{0, \dots, M-1\} \end{aligned} \quad (5)$$

In the following, we examine several methods for solving this problem and enforcing $N : M$ transposable fine-grained sparsity during training. We first describe an optimal, yet computationally expensive method. Then we describe a more efficient method, yet only provides an approximate, though near-optimal, solution.

4.2. Reduction to Min-Cost Flow

General integer programs (IP) have exponential time complexity with respect to the input size (worst-case). Fortunately, Fig. 4 showed that our IP formulation at Eq. (5) can be reduced to a min-cost flow problem. Hence, by using *cost-scaling* method to solve the problem (Ahuja et al., 1988), we can find the optimal transposable mask in $O(M^3 \log(M))$ time for a block size of $M \times M$.

The min-cost flow solution should be used when training from a pretrained dense model (Section 6.1), where the transposable mask is generated once and is then fixed during training. Sparse training from scratch on the other hand, requires changing the mask during training (Section 6.2). Therefore it is essential to find a very efficient algorithm for computing the mask. To that end we design a light *2-approximation* algorithm, i.e., for every input it produces a solution which is guaranteed to be within a factor of 2 of an optimal solution (to the input), yet it runs in almost linear time.

2-approximation algorithm: We design a greedy *2-approximation* algorithm (see Algorithm 1) having a low

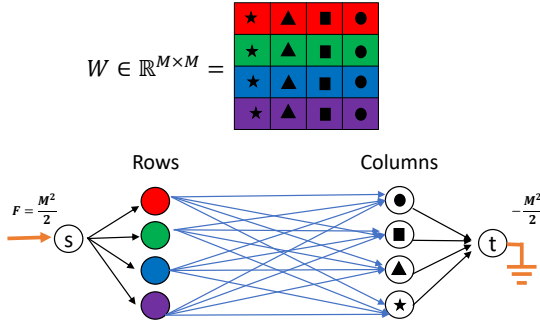


Figure 4. $\frac{M}{2} : M$ transposable-sparsity optimization as a min-cost flow problem. In addition to a source and a sink, the network has a node for each row and for each column. The construction uses three types of edges: (i) *source edges* emanating from the source node s into each row node i ; (ii) *sink edges* connecting each column node j with the sink node t ; and (iii) a *coefficient edge* (i, j) for each matrix element $W_{i,j}$. Each source edge (si) has capacity $\frac{M}{2}$ which is equal to the number of elements that need to be selected for pruning in row i . Similarly, each sink edge (jt) has capacity $\frac{M}{2}$ which is equal to the number of elements pruned in column j . Each coefficient edge (ij) has unit capacity and cost $|W_{i,j}|$. Finally, selecting a matrix element with weight $W_{i,j}$ for pruning corresponds to a unit flow on the coefficient edge (ij) . A min-cost flow from source s to destination t would find the lowest possible cost of sending a flow of value $\frac{M^2}{2}$ from the source s to the destination t . Assuming the source and sink edges have a zero cost, it is easy to see a one-to-one correspondence between a min-cost flow in this construction and an optimal transposable mask, that minimizes the sum of absolute values selected for pruning.

time complexity that can be used in practice without compromising too much the quality of the solution produced. Unlike the optimal min cost flow solution that runs in time complexity of $O(M^3)$ for a block size of $M \times M$, Algorithm 1 has a running time of $O(M^2 \log M)$ i.e., a time complexity that is almost linear in the number of block elements M^2 . The approximation algorithm uses the same construction described in Fig. 4, but instead of running a min-cost flow on the graph, it employs a simple greedy approach. In Appendix A.3 we analyze the running times of different min-cost flow methods and compare them with the running time of our 2-approximation method.

Let P be the list of edges pruned by Algorithm 1, let $W(P)$ be the total weight of the edges in P , and let W^* be the weight of an optimal solution (i.e., the minimal sum of edges that can be pruned to create a $\frac{M}{2} : M$ transposable sparsity mask). The next lemma establishes that Algorithm 1 finds a 2-approximate solution.

Lemma. *Algorithm 1 produces a tight 2-approximate solution, i.e., $W(P) < 2 \cdot W^*$.*

Proof. Consider any node $i \in V \setminus \{s, t\}$. Let $E'(i) = \{e'_1, e'_2, e'_3, \dots, e'_{M/2}\}$ denote the edges of an optimal solution that are adjacent to node i and sorted in ascending order from light to heavy. Let $E(i) = \{e_1, e_2, e_3, \dots, e_{M/2}\}$ denote the first $M/2$ edges adjacent to i in P with respect to the order in which Algorithm 1 picked them. By construction, we have that for all edges in $E(i)$:

$$w(e_1) \leq w(e_2) \dots \leq w(e_{M/2}). \quad (6)$$

We note that we can truncate the list of i at $M/2$, since if i has more than $M/2$ edges adjacent to it in P , then any such edge (i, j) would also appear in $E(j)$ (among the first $M/2$ edges adjacent to j). Thus, the union of the lists $E(i)$ contains all edges in P . We now prove by induction that for any $n, n \geq 1$,

$$w(e_n) \leq w(e'_n). \quad (7)$$

- **Base case ($n = 1$):** $w(e_1) \leq w(e'_1)$, since by construction of Algorithm 1, edge e_1 is the lightest edge adjacent to node i .
- **Induction step:** assume $w(e_n) \leq w(e'_n)$, then it must hold that $w(e_{n+1}) \leq w(e'_{n+1})$; otherwise, if $w(e_{n+1}) > w(e'_{n+1})$, then e'_{n+1} should have been considered before e_{n+1} and also chosen by Algorithm 1.

Thus,

$$\sum_{j=1}^{M/2} w(e_j) \leq \sum_{j=1}^{M/2} w(e'_j).$$

To complete the proof, our goal is to change the weight of the edges in P to the weight of the edges in the optimal solution based on the above inequality. However, note that an edge $(i, j) \in P$ may appear in only one of the lists $E(i)$ or $E(j)$, while an edge in the optimal solution always appears in two lists (of its endpoints). Thus, for example, two edges in P , (i, j) and (i', j) , may charge their weight to the same edge (i, i') in the optimal solution. But, this "double" charging can happen at most twice, hence:

$$W(P) \leq 2W^*. \quad (8)$$

In Appendix A.2 we show with an example that this upper bound is tight. ■

5. Mask Diversity

Structure sparsity requires the mask to have some hardware-friendly pattern. In this section, we will argue that the more flexible the required sparsity constraint is (e.g., fine-grained sparsity with large block) the less we are prone to accuracy degradation. Consequently, as expected and well explored

Algorithm 1 2- approximation algorithm

Input: Graph $G=(V,E)$
 Initialize $P=\emptyset$
 Sort the list of coefficient edges from light to heavy
 Let $A = [e_1, \dots, e_n]$ be the sorted list of edges
for each edge $e_i = (u, v) \in A$ **do**
 if $\text{degree}(u) \leq \frac{M}{2}$ or $\text{degree}(v) \leq \frac{M}{2}$ in P **then**
 $P \leftarrow P + e_i.$
end if
end for

(Frankle & Carbin, 2018; Renda et al., 2020b), unstructured sparsity which has no requirements on the sparsity structure achieves the best sparsity levels. To quantify the constraint a specific mask enforces, we introduce a new measure we name *mask-diversity*. A mask diversity (MD) is the number of all possible configurations which adhere to the mask restriction under similar sparsity level.

Let us consider W to be a weight tensor of size $n \times n$ and our desired sparsity level to be N/n^2 . For unstructured sparsity

$$MD_{\text{Unstructured}} = \binom{n^2}{N} \quad (9)$$

As the block size increases, the diversity increases, which might explain the recent success of global pruning. Here we investigate per-layer block sparsity and specifically, fine-grained $N : M$ structured sparsity (Nvidia, 2020). This approach requires us to zero out N values in each block of size M . Since we have $\frac{n^2}{M}$ blocks this results in

$$MD_{\text{Structured}} = \left(\frac{M!}{N!(M-N)!} \right)^{\frac{n^2}{M}}. \quad (10)$$

In order to evaluate the mask diversity in the $N : M$ structured transposable case, let us first assume $N = 1$. The number of possibilities in each block of size M^2 is $M!$. By repeating this process for general N in all the $\frac{n^2}{M^2}$ blocks we get:

$$MD_{\text{Structured transposable}} = (M!(M-1)! \cdots (M-N+1)!)^{\frac{n^2}{M^2}} \quad (11)$$

A more constrained mask, is a fine-grained $N : M$ mask with a sequential structure. Here we require that each M contiguous elements would contain N sequential zeros. In each block of size M^2 , there are $(M-N+1)^M$ options of sequential zeros. Hence, in all the $\frac{n^2}{M^2}$ blocks we get:

$$MD_{\text{Sequential}} = ((M-N+1)^M)^{\frac{n^2}{M^2}} \quad (12)$$

In Table 1 we show the MD for different constraints for a matrix of size 8×8 . Notice the diversity of structured

 Table 1. MD for different constraints for a matrix of size 8×8 .

$N : M$	1:2	2:4	4:8
Unstructured	$1.8 \cdot 10^{18}$	$1.8 \cdot 10^{18}$	$1.8 \cdot 10^{18}$
Structured	$4 \cdot 10^9$	$2.8 \cdot 10^{12}$	$5.7 \cdot 10^{14}$
Transposable structured	$6 \cdot 10^4$	$4 \cdot 10^8$	$1.7 \cdot 10^{13}$
Sequential	$4 \cdot 10^9$	$4 \cdot 10^7$	$4 \cdot 10^5$

2:4, which was used in Nvidia (2020); Zhou et al. (2021) is similar to the transposable structured 4:8. In Fig. 5 we show the l_1 norm of the last layer in trained ResNet-50 masked with different structured pruning. We note that 2:4 structured and 4:8 transposable structured have (almost) similar MD measures which translates to similar l_1 norms as well. In order to show the correlation between MD and

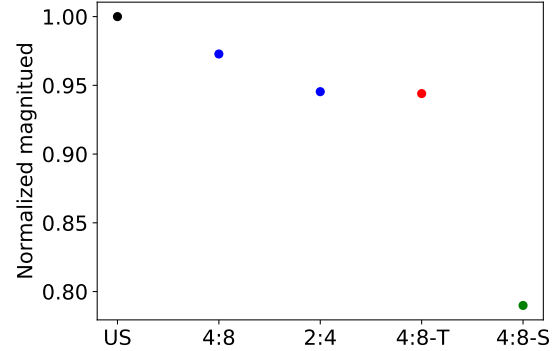


Figure 5. Magnitude of the last layer’s weight tensor of ResNet-50 (pretrained dense model) masked with structured mask 4:8, 2:4, 4:8 transposable (“4:8-T”) and 4:8 sequential (“4:8-S”) normalized by the unstructured 50% sparsity (“US”). Notice that mask diversity is correlated with magnitude preservation. As expected the 4:8 transposable mask has a similar L1 score as the 2:4 mask.

the accuracy of the model, we show in Fig. 6 the accuracy of ResNet18 on Cifar100 dataset while inducing different sparsity masks with the same sparsity ratio of 50%. As expected, our mask-diversity measure correlates with the pruned model accuracy.

6. Experiments

In this section, we demonstrate the effectiveness of our proposed transposable $N : M$ fine-grained structured sparsity in computer vision and natural language processing tasks. We compare the suggested method over two different initialization: (i) initialization from a trained dense model and train with a fixed mask, similar to ASP (Nvidia, 2020), (ii) Train from scratch and update the mask frequently, simi-

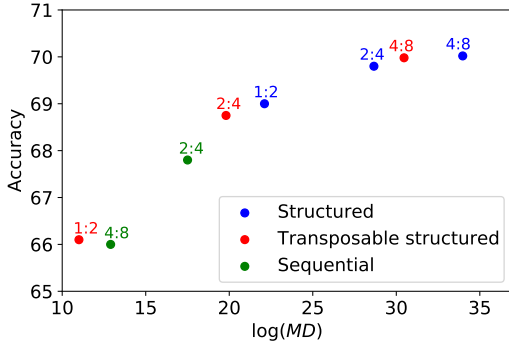


Figure 6. ResNet18 on Cifar100 accuracy for weight sparsity of 50% using different structured mask. Notice that the more constraints we impose on the mask - the more we affect the pruned network accuracy.

lar to Zhou et al. (2021). We show comparable accuracy to previous methods, while achieving a significant reduction of the training process resources — by exploiting the sparse core tensor abilities, allowing their use both in forward and backward passes. In all the experiments we use a transposable 4:8 mask, which as shown in Table 1, have a similar MD as 2:4 mask used in previous works (Nvidia, 2020; Zhou et al., 2021). Experiments setting appears in Appendix A.4

6.1. Initialization from a trained dense model

We evaluate the suggested $N : M$ transposable mask using a trained dense model as initialization. In order to find the transposable mask, we solve the min-cost flow reduction (Section 4.2) on the dense trained network and then fix the mask. In Table 2 we compare our method with ASP (Nvidia, 2020) on classification (ResNet50 - ImageNet dataset), detection (MaskRCNN - COCO dataset) and question answering (BERT-large - SQuAD dataset) tasks. Notice that the initialization in both methods is similar, however, in the training phase, we allow 2x acceleration by the use of the 4:8 transposable mask in comparison to the 2:4 non transposable used in ASP.

6.2. Sparse Training from scratch

In order to avoid the training of a dense model, we also evaluate the proposed transposable $N : M$ mask in the training from scratch setting. Similar to Zhou et al. (2021) we keep a dense copy of the weights and before each forward pass we mask the weights with a $N : M$ transposable mask. In contrast to Zhou et al. (2021) who changed the mask every iteration, we found that we can use 2-approximation scheme to extract the transposable mask every 40 iterations. Empirically we found that the 2-approximation scheme is

Table 2. Comparison of the suggested method with ASP (Nvidia, 2020) initialized from dense model on ResNet50 (Imagenet dataset), BERT-large (SQuAD dataset) and MaskRCNN (COCO dataset). We use transposable 4:8 mask while ASP use 2:4. The use of the transposable mask allow 2x speedup by allowing sparse multiplication both in forward and backward passes.

Model (Metric)	Method	Accuracy	Sparse core utilization
ResNet18 (Top1)	Baseline	69.7%	0%
	Ours	70.06	66%
ResNet50 (Top1)	Baseline	76.15%	0%
	ASP	76.6%	33%
	Ours	76.6%	66%
	BERT-large (F1)	Baseline	91.1
ASP		91.5	33%
	Ours	91.67	66%
	MaskRCNN (AP)	Baseline	37.7
ASP		37.9	33%
	Ours	37.84	66%

on average within a factor of 1.2 from the optimal mask. The hyper-parameters used for training are equal to the ones suggested by Zhou et al. (2021). In Table 3 we test the proposed method over ResNet18, ResNet50, ResNext50, Vgg11 (ImageNet dataset) and fine-tune of Bert (SQuAD-v1.1 dataset) and compare to Zhou et al. (2021) results. As can be seen, we achieved comparable accuracy with 2x speedup in the training process.

7. Conclusions

In this work, we analyze the constraints introduced by block sparsity. We discuss the limitations with current research in the field and suggest two simple methods (Pruning bias fix and AdaPrune) to transform an unstructured sparse model to a fine-grained sparse structured model with little to no training. We managed to reduce accuracy degradation caused by forcing $N : M$ pattern on unstructured sparse mask. As an example, in ResNet50 we reduce the degradation to less than 1% from the unstructured model without any retraining. Furthermore, with a light training procedure over a calibration set (i.e., AdaPrune) we can compress the model by up to x3.

In addition, we discuss the inherent problem of accelerating sparse training and suggest a novel N:M transposable mask which enables accelerating the backward phase as well. We formulate the question of finding the optimal mask as a minimum-cost-flow problem and show no accuracy degradation in a variety of tasks with 2x acceleration in comparison to previous methods (Nvidia, 2020). Moreover, we design a new fast algorithm (with linear complexity)

Table 3. Training from scratch of ResNet18, ResNet50, ResNext50 and Vgg11 on imageNet dataset and fine-tuning of Bert-base on SQuAD dataset, using the proposed 2-scheme approximation. We show comparable results with N:M-SS (Zhou et al., 2021) with training acceleration.

Model (Metric)	Method	Accuracy	Sparse core utilization
ResNet18 (Top1)	Baseline	70.54%	0%
	N:M-SS	71.2%	33%
	Ours	70.75%	66%
ResNet50 (Top1)	Baseline	77.3%	0%
	N:M-SS	77.4%	33%
	Ours	77.1%	66%
ResNext50 (Top1)	Baseline	77.6%	0%
	Ours	77.4%	66%
Vgg11 (Top1)	Baseline	69%	0%
	Ours	68.8%	66%
BERT-base (F1)	Baseline	88.52	0%
	Ours	88.38	66%

that guarantees to be within a factor of 2 from the optimal transposable mask L1 norm and use it to train a sparse model from scratch by accelerating both forward and backward phases. We believe this work paves the path toward true efficient sparse training.

References

- Ahuja, R. K., Magnanti, T. L., and Orlin, J. B. Network flows. 1988.
- Banner, R., Hubara, I., Hoffer, E., and Soudry, D. Scalable methods for 8-bit training of neural networks. In *NeurIPS*, 2018a.
- Banner, R., Nahshan, Y., Hoffer, E., and Soudry, D. Post-training 4-bit quantization of convolution networks for rapid-deployment. *arXiv preprint arXiv:1810.05723*, 2018b.
- Bellec, G., Kappel, D., Maass, W., and Legenstein, R. Deep rewiring: Training very sparse deep networks. *arXiv preprint arXiv:1711.05136*, 2017.
- Bengio, Y., Léonard, N., and Courville, A. Estimating or propagating gradients through stochastic neurons for conditional computation. *arXiv preprint arXiv:1308.3432*, 2013.
- Brown, T., Mann, B., Ryder, N., Subbiah, M., Kaplan, J., Dhariwal, P., Neelakantan, A., Shyam, P., Sastry, G., Askell, A., Agarwal, S., Herbert-Voss, A., Krüger, G., Henighan, T., Child, R., Ramesh, A., Ziegler, D., Wu, J., Winter, C., Hesse, C., Chen, M., Sigler, E., Litwin, M., Gray, S., Chess, B., Clark, J., Berner, C., McCandlish, S., Radford, A., Sutskever, I., and Amodei, D. Language models are few-shot learners. *ArXiv*, abs/2005.14165, 2020.
- Dettmers, T. and Zettlemoyer, L. Sparse networks from scratch: Faster training without losing performance. *arXiv preprint arXiv:1907.04840*, 2019.
- Evci, U., Gale, T., Menick, J., Castro, P. S., and Elsen, E. Rigging the lottery: Making all tickets winners. In *International Conference on Machine Learning*, pp. 2943–2952. PMLR, 2020.
- Fedus, W., Zoph, B., and Shazeer, N. Switch transformers: Scaling to trillion parameter models with simple and efficient sparsity. *ArXiv*, abs/2101.03961, 2021.
- Finkelstein, A., Almog, U., and Grobman, M. Fighting quantization bias with bias. *arXiv preprint arXiv:1906.03193*, 2019.
- Frankle, J. and Carbin, M. The lottery ticket hypothesis: Finding sparse, trainable neural networks. In *ICLR*, 2018.
- Gray, S., Radford, A., and Kingma, D. P. Gpu kernels for block-sparse weights. *arXiv preprint arXiv:1711.09224*, 3, 2017.
- Han, S., Pool, J., Tran, J., and Dally, W. Learning both weights and connections for efficient neural network. *ArXiv*, abs/1506.02626, 2015.
- He, K., Zhang, X., Ren, S., and Sun, J. Deep residual learning for image recognition. *2016 IEEE Conference on Computer Vision and Pattern Recognition (CVPR)*, pp. 770–778, 2016.
- Hinton, G. E., Vinyals, O., and Dean, J. Distilling the knowledge in a neural network. *ArXiv*, abs/1503.02531, 2015.
- Hubara, I., Courbariaux, M., Soudry, D., El-Yaniv, R., and Bengio, Y. Quantized neural networks: Training neural networks with low precision weights and activations. *The Journal of Machine Learning Research*, 18(1):6869–6898, 2017.
- Hubara, I., Nahshan, Y., Hanani, Y., Banner, R., and Soudry, D. Improving post training neural quantization: Layer-wise calibration and integer programming. *ArXiv*, abs/2006.10518, 2020.
- Janowsky, S. A. Pruning versus clipping in neural networks. *Physical Review A*, 39(12):6600–6603, 1989. URL <https://link.aps.org/doi/10.1103/PhysRevA.39.6600>.

- Karnin, E. D. A simple procedure for pruning backpropagation trained neural networks. *IEEE transactions on neural networks*, 1(2):239–242, 1990.
- Lee, N., Ajanthan, T., and Torr, P. Snip: Single-shot network pruning based on connection sensitivity. In *ICLR*, 2019.
- Li, H., Kadav, A., Durdanovic, I., Samet, H., and Graf, H. P. Pruning filters for efficient convnets. In *ICLR*, 2017.
- Liu, Z., Sun, M., Zhou, T., Huang, G., and Darrell, T. Rethinking the value of network pruning. *arXiv preprint arXiv:1810.05270*, 2018.
- Louizos, C., Welling, M., and Kingma, D. P. Learning sparse neural networks through l0 regularization. In *ICLR*, 2018.
- Luo, J.-H., Wu, J., and Lin, W. Thinet: A filter level pruning method for deep neural network compression. *2017 IEEE International Conference on Computer Vision (ICCV)*, pp. 5068–5076, 2017.
- Marcel, S. and Rodriguez, Y. Torchvision the machine-vision package of torch. In *Proceedings of the 18th ACM International Conference on Multimedia*, MM '10, pp. 1485–1488, New York, NY, USA, 2010. Association for Computing Machinery. ISBN 9781605589336. doi: 10.1145/1873951.1874254. URL <https://doi.org/10.1145/1873951.1874254>.
- Mocanu, D. C., Mocanu, E., Stone, P., Nguyen, P. H., Gibescu, M., and Liotta, A. Scalable training of artificial neural networks with adaptive sparse connectivity inspired by network science. *Nature communications*, 9(1):1–12, 2018.
- Mostafa, H. and Wang, X. Parameter efficient training of deep convolutional neural networks by dynamic sparse reparameterization. In *International Conference on Machine Learning*, pp. 4646–4655. PMLR, 2019.
- Mozer, M. C. and Smolensky, P. Skeletonization: A technique for trimming the fat from a network via relevance assessment. *Advances in neural information processing systems*, pp. 107–115, 1989a.
- Mozer, M. C. and Smolensky, P. Using relevance to reduce network size automatically. *Connection Science*, 1(1):3–16, 1989b.
- Nagel, M., Amjad, R. A., van Baalen, M., Louizos, C., and Blankevoort, T. Up or down? adaptive rounding for post-training quantization. In *ICML*, 2020.
- Nahshan, Y., Chmiel, B., Baskin, C., Zheltonozhskii, E., Banner, R., Bronstein, A. M., and Mendelson, A. Loss aware post-training quantization. *ArXiv*, abs/1911.07190, 2019.
- Nvidia. Nvidia deep learning examples for tensor cores. 2018. URL <https://github.com/NVIDIA/DeepLearningExamples/tree/master/PyTorch>.
- Nvidia. a100 tensor core gpu architecture. 2020. URL <http://https://www.nvidia.com/content/dam/en-zz/Solutions/Data-Center/nvidia-ampere-architecture-whitepaper.pdf>.
- Renda, A., Frankle, J., and Carbin, M. Comparing rewinding and fine-tuning in neural network pruning. *ArXiv*, abs/2003.02389, 2020a.
- Renda, A., Frankle, J., and Carbin, M. Comparing rewinding and fine-tuning in neural network pruning. In *ICLR*, 2020b.
- Tan, M., Chen, B., Pang, R., Vasudevan, V., Sandler, M., Howard, A., and Le, Q. V. Mnasnet: Platform-aware neural architecture search for mobile. In *Proceedings of the IEEE/CVF Conference on Computer Vision and Pattern Recognition*, pp. 2820–2828, 2019.
- Wen, W., Wu, C., Wang, Y., Chen, Y., and Li, H. Learning structured sparsity in deep neural networks. In *In Advances in neural information processing systems*, pp. 2074–2082, 2016.
- Wu, B., Dai, X., Zhang, P., Wang, Y., Sun, F., Wu, Y., Tian, Y., Vajda, P., Jia, Y., and Keutzer, K. Fbnet: Hardware-aware efficient convnet design via differentiable neural architecture search. In *Proceedings of the IEEE/CVF Conference on Computer Vision and Pattern Recognition*, pp. 10734–10742, 2019.
- Zhou, A., Ma, Y., Zhu, J., Liu, J., Zhang, Z., Yuan, K., Sun, W., and Li, H. Learning n:m fine-grained structures sparse neural networks from scratch. In *ICLR*, 2021.

A. Supplementary Material

A.1. Additional AdaPrune experiments

To further examine AdaPrune capabilities we checked two additional settings: (a) starting from pre-trained dense model, and (b) starting from less constrained N:M mask.

A.1.1. ADAPRUNE FROM DENSE

While this case is more common, we expect to see some degradation as we know that we have 50% mask violations. Yet as can be seen in table 2 we managed to restore accuracy to 2-3% of the full-precision baseline using just AdaPrune. To further improve results we applied batch-norm-tuning as suggested by Hubara et al. (2020) and kept the first and last layers dense which results in less than 2% degradation. We believe it to be the first tolerable post-training-pruning results reported.

Table A.1. Using AdaPrune from dense pre-trained model. AP stands for AdaPrune and BNT stands for batch-norm-tuning.

Model	Dense	BiasFix BNT	AP	AP BNT
ResNet18	69.7%	62.47%	68.41%	68.63%
ResNet34	73.3% %	68.72%	72.15%	72.36%
ResNet50	76.1%	67.42%	74.41	74.75%
ResNet101	77.27 %	71.54%	76.36%	76.48%

A.1.2. ADAPRUNE FROM N:M SPARSE

In Section 5 we explained why as the block size decreases the mask diversity decreases. Thus, we expect to have many violations when a pre-trained sparse model with $N_1 : M_1$ translates to $N_2 : M_2$, for $N_1 > N_2$ and $M_1 > M_2$. We argue that this might be a common case in the future as different hardware vendors would support different formats. In table Table A.2 we can see results of converting ResNet-50 model trained with 4 : 8 sparsity pattern to 2 : 4 and 1 : 2 patterns. As can be seen, converting from 4 : 8 to 2 : 4 produces results with negligible accuracy degradation (less than 0.5%). Therefore, we argue that AdaPrune is an efficient and useful approach to convert models which were optimized on a different hardware than the one in use, as it removes the need for full sparse training. This is even more important when the training data is not available.

A.2. A tight example for the 2-approximation factor in Lemma

In the following, we show that the upper bound of 2-approximation (proven in Lemma) is asymptotically tight using a tight example. Let’s assume we want to zero one element in each row and column in the block of size 4×4

Table A.2. Using AdaPrune to convert from one sparse pattern to the other. The baseline model was trained with 4:8 sparsity (90 epochs). Thus, 4:8 column is the baseline. BNT stands for batch-norm-tuning

Model	4:8	2:4	2:4 BNT	1:2	1:2 BNT
RN50	76.5%	76.2%	76.4%	74.6%	75.1%
RN50-T	77.1%	76.3%	76.4%	74.7%	75.1%
RN18-T	70.75%	70.1%	70.2%	68.9%	69.2%

presented in Fig. A.1a using 2-approximate algorithm (Algorithm 1). First, we need to convert the block into a direct bipartite graph (as suggested in Figure 4). This construction appears in Fig. A.1b. Next, we sort the edges from light to heavy and go over the sorted list. In Fig. A.1c we show the 7th iteration of the 2-approximate algorithm. All edges are added to the list of chosen edges P up until iteration 7. The algorithm stops at iteration 7 since after adding the link $u_1 \xrightarrow{1} v_1$, every node is "covered" by at least one edge (alternatively, each row and each column has at least one item chosen for pruning). Note that the optimal solution would choose the edges that correspond to elements on the diagonal (i.e., $u_1 \xrightarrow{1} v_1, u_2 \xrightarrow{1} v_2, u_3 \xrightarrow{1} v_3$, and $u_4 \xrightarrow{1} v_4$), summing to a total weight of 4. Hence, we get an approximation ratio of $\frac{7}{4}$. It is easy to see that when using the same construction for a general block of size $M \times M$ we get an approximation ratio of $\frac{2M-1}{M}$, asymptotically converging to 2 as $M \rightarrow \infty$.

A.3. Run-time analysis

In this section we specify the running times of different min-cost flow methods and compare them with the running time of our 2-approximation method. Ahuja et al. (1988) specifies the running times of six min-cost flow algorithms, two of which have distinctively better performance for our construction compared to the others. The running time complexities of these two methods depend on the following parameters: number of nodes n , number of edges m , the largest weight coefficient W , and the flow demand U . Then, the *cost-scaling method* has a running time of $\mathcal{O}(n^3 \log(n \cdot W))$ while the *capacity scaling method* has a running time of $\mathcal{O}(m(m + n \log n) \log U)$. For a block of size $M \times M$, our construction process creates a number of edges $m = M^2 + 2M$, a number of nodes $n = 2M + 2$, and a flow demand $U = 0.5M^2$. This boils down to running times of $\mathcal{O}(M^3 \log(M \cdot W))$ and $\mathcal{O}(M^4 \log(M))$ for the cost-scaling and the capacity-scaling methods, respectively. Finally, assuming the weights are represented in b bits, we have that $\log(W) = b$ and therefore solving our construction using the cost-scaling method has a running time complexity of $\mathcal{O}(M^3(\log(M) + b))$. In Table A.3 we

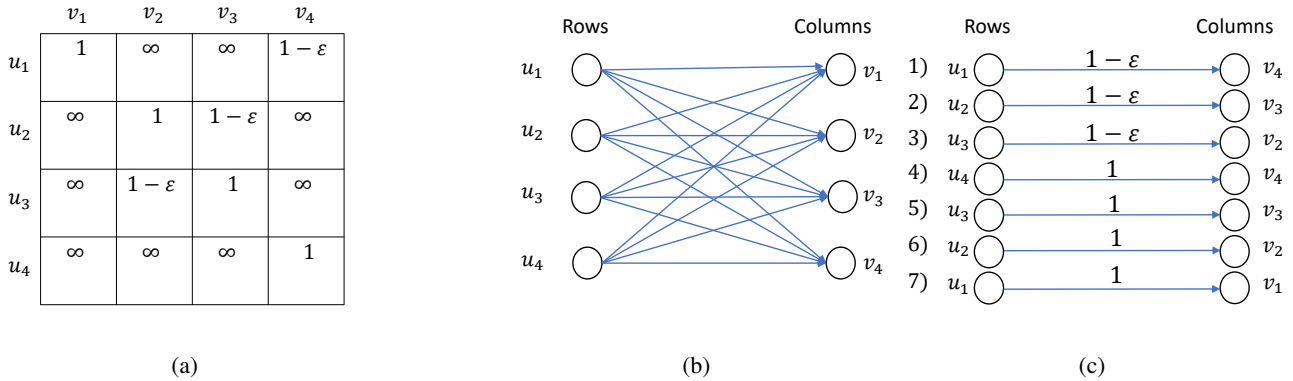


Figure A.1. (a): Block of size 4×4 where we want to zero one element in each row and column using 2-approximate algorithm. (b): Block in (a) represented in a direct bipartite graph. (c): The 7 iterations of the 2-approximate algorithm on graph (b). Notice we get an approximate ratio between the 2-approximate solution and the optimal solution of $\frac{7}{4}$.

Table A.3. Running times of min-cost flow based implementations and the 2-approximation method.

Method	Complexity
Cost-Scaling	$\mathcal{O}(M^3(\log(M) + b))$
Capacity-Scaling	$\mathcal{O}(M^4 \log(M))$
2-approximation	$\mathcal{O}(M^2 \log(M))$

summarize the complexity of these methods.

A.4. Experiments Setting

AdaPrune We used a small calibration set of 1000 images (one per-class). We run AdaPrune for 1000 iterations with batch-size of 100. For the results in the supplementary material, we kept the first and last layers dense.

N:M transposable sparsity mask from a pre-trained model We used torchvision (Marcel & Rodriguez, 2010) model-zoo as our pre-trained dense baseline. For all ResNet models we used the original regime as given by He et al. (2016), i.e., SGD over 90 epochs starting with learning rate of 0.1 and decreasing it at epochs 30,60,80 by a factor of 10. For BERT-large and MaskRCNN we used the defaults scripts as in Nvidia (2018).

N:M transposable sparsity mask from scratch We use the exact same setting as given by Zhou et al. (2021).